Atmos. Chem. Phys. Discuss., 15, 35907–35938, 2015
www.atmos-chem-phys-discuss.net/15/35907/2015/
doi:10.5194/acpd-15-35907-2015

Atmospheric Chemistry and Physics Discussions

What controls the low ice number concentration in the upper troposphere?

C. Zhou[1], J. E. Penner[1], G. Lin[1,a], X. Liu[2], and M. Wang[3,4]

[1]University of Michigan, Ann Arbor, MI, USA
[2]University of Wyoming, Laramie, WY, USA
[3]Institute for Climate and Global Change Research & School of Atmospheric Sciences, Nanjing University, Nanjing, 210023, China
[4]Collaborative Innovation Center of Climate Change, Jiangsu Province, China
[a]now at: Pacific Northwest National Laboratory, Richland, Washington, USA

Received: 10 December 2015 – Accepted: 11 December 2015
– Published: 21 December 2015

Correspondence to: C. Zhou (zhouc@umich.edu)

Published by Copernicus Publications on behalf of the European Geosciences Union.

Abstract

Cirrus clouds in the tropical tropopause play a key role in regulating the moisture entering the stratosphere through their dehydrating effect. Low ice number concentrations ($< 200\,L^{-1}$) and high supersaturations (150–160 %) have been observed in these clouds. Different mechanisms have been proposed to explain these low ice number concentrations, including the inhibition of homogeneous freezing by the deposition of water vapour onto pre-existing ice crystals, heterogeneous ice formation on glassy organic aerosol ice nuclei (IN), and limiting the formation of ice number from high frequency gravity waves. In this study, we examined the effect from three different representations of updraft velocities, the effect from pre-existing ice crystals, the effect from different water vapour deposition coefficients ($\alpha = 0.1$ or 1), and the effect of 0.1 % of the total secondary organic aerosol (SOA) particles acting as IN. Model simulated ice crystal numbers are compared against an aircraft observational dataset.

Including the effect from water vapour deposition on pre-existing ice particles can effectively reduce simulated in-cloud ice number concentrations for all model set-ups. A larger water vapour deposition coefficient ($\alpha = 1$) can also efficiently reduce ice number concentrations at temperatures below 205 K but less so at higher temperatures. SOA acting as IN are most effective at reducing ice number concentrations when the effective updraft velocities are moderate (~ 0.05–$0.2\,m\,s^{-1}$). However, the effects of including SOA as IN and using ($\alpha = 1$) are diminished when the effect from pre-existing ice is included.

When a grid resolved large-scale updraft velocity ($< 0.1\,m\,s^{-1}$) is used, the ice nucleation parameterization with homogeneous freezing only or with both homogeneous freezing and heterogeneous nucleation is able to generate low ice number concentrations in good agreement with observations for temperatures below 205 K as long as the pre-existing ice effect is included. For the moderate updraft velocity (~ 0.05–$0.2\,m\,s^{-1}$) simulated ice number concentrations in good agreement with observations at temperatures below 205 K can be achieved if effects from pre-existing ice, a larger water vapour

ACPD
15, 35907–35938, 2015

deposition coefficient (α = 1) and SOA IN are all included. Using the sub-grid scale turbulent kinetic energy based updraft velocity ($\sim$ 0–2 m s^{-1}) always overestimates the ice number concentrations at temperatures below 205 K but compares well with observations at temperatures above 205 K when the pre-existing ice effect is included.

1 Introduction

Cirrus clouds cover about 30 % of the Earth's area (Wang et al., 1996; Rossow and Schiffer, 1999; Wylie and Menzel, 1999) and are important in maintaining the global radiation balance (Ramanathan and Collins, 1991). They warm the atmosphere by absorbing outgoing longwave radiation emitted by the Earth and atmosphere and re-emitting it at much lower temperatures. This warming effect is partly compensated by their reflection of incoming solar radiation. Cirrus clouds also control the dehydration of air before its entry into the stratosphere (Jensen et al., 1996, 2013). Their radiative impacts, ability to affect water vapour cycles, and cirrus cloud evolution are sensitive to the ice number concentration. Ice in cirrus clouds can form through either homogeneous freezing of supercooled aqueous solutions (Koop et al., 2000) which typically generates high ice number concentrations or heterogeneous nucleation of different modes (deposition, contact, immersion, and condensation) triggered by insoluble aerosol particles (which are termed heterogeneous ice nuclei, IN) (Pruppacher and Klett, 1997). Heterogeneous nucleation typically forms much lower ice number concentrations due to the limited IN concentration in the atmosphere (Rogers et al., 1998).

Low ice number concentrations ($< 200\,\mathrm{L}^{-1}$) and high in-cloud ice supersaturations (150–160 %) are frequently observed near the tropical tropopause layer (TTL) (e.g. Krämer et al., 2009; Jensen et al., 2010, 2013). The observed high in-cloud ice supersaturations are consistent with the long relaxation times needed to remove the excess water vapour above ice saturation by deposition due to low ice number concentrations. These low ice numbers are not consistent with the conventional theory of ice nucleation via homogenous freezing at the cold temperatures in the TTL (e.g. Krämer et al., 2009;

ACPD
15, 35907–35938, 2015

Jensen et al., 2010) if a typical value of temperature fluctuation or updraft velocity is used.

Various proposals have been put forward to explain the low ice number concentrations in the TTL. These can largely be divided into 3 categories. The first category is inhibition of homogeneous freezing by heterogeneous IN (e.g. Abbatt et al., 2006; Murray et al., 2010) or pre-existing ice particles (e.g. Kuebbeler et al., 2014; Shi et al., 2015). Abbatt et al. (2006) showed that solid ammonium sulphate aerosols can be effective heterogeneous ice nuclei at cirrus temperatures and lead to fewer but larger ice crystals compared to a homogeneous freezing scenario. Murray et al. (2010) showed that organic matter can become glassy under cirrus conditions and thereby become heterogeneous IN. Thus the low ice number and high RHi could be explained by heterogeneous nucleation of ice on glassy solution droplets. Kuebbeler et al. (2014) studied the effect of vapour deposition onto pre-existing ice during nucleation, which can prevent high supersaturations and thereby prevent either homogeneous or heterogeneous freezing from occurring. They found that the effect of pre-existing ice together with heterogeneous nucleation on mineral dust particles can significantly reduce global ice crystal number and mass. Shi et al. (2015) also found that the inclusion of vapour deposition onto pre-existing ice during nucleation significantly reduces ice number concentrations in cirrus clouds, especially at middle to high latitudes in the upper troposphere (by a factor of ~ 10).

The second category of proposals that might explain the observed low ice number concentrations in the TTL is related to gravity wave cycles (e.g. Spichtinger and Krämer 2013; Dinh et al., 2015). In most ice nucleation parameterizations, it is often assumed that the relevant time scale for ice nucleation (i.e., a few minutes) is sufficiently short such that the vertical velocity and associated adiabatic cooling rate remain constant (e.g. Liu and Penner, 2005; Kärcher et al., 2006; Barahona and Nenes, 2008). For the above proposals in the second category to form low ice numbers ($< 200\,\mathrm{L}^{-1}$) the constant cooling rate or updraft velocity has to be low enough (several cm s^{-1}). However, vertical velocity measurements from the Interhemispheric Differences in Cirrus Prop-

ACPD
15, 35907–35938, 2015

erties From Anthropogenic Emissions (INCA) campaign indicate that updraft velocities higher than 0.2 m s^{-1} are often observed (Kärcher and Ström, 2003). Spichtinger and Krämer (2013) studied the effect of the superposition of a slow large-scale updraft with a high-frequency, short wavelength gravity wave. Under these circumstances, the observed TTL low cirrus ice numbers could be explained by "classical" homogeneous ice nucleation. They show model simulations of homogenous freezing starting at the tip of the high frequency wave just before it is about to turn from an upward movement to a downward movement. Consequently the amount of time available for homogenous freezing event is substantially limited due to the downdraft, and hence the newly formed ice number from homogeneous freezing is also reduced. They suggest that large-scale models would reproduce their results just by using the large-scale updraft velocity in ice nucleation parameterizations. Dinh et al. (2015) studied homogeneous ice nucleation using a parcel model with observed temperature time series from balloon flights near the tropical tropopause. They showed that low ice number concentrations can also be obtained if the gravity wave perturbations produce a non-persistent cooling rate such that the absolute change in temperature remains small during ice nucleation events.

The third category of proposals that might explain the observed low ice number concentrations in the TTL is related to the sedimentation of ice particles (e.g. Barahona and Nenes, 2011; Murphy, 2014). Barahona and Nenes (2011) showed that the dynamical balance between new ice particle production and sedimentation can set the cirrus clouds into one of two "preferred" microphysical regimes based on the magnitude of the temperature fluctuations. For small temperature fluctuations, the balance between the formation of ice crystals from homogeneous freezing and sedimentation was able to explain low ice number concentrations, although this finding could not be confirmed in the study by Jensen et al. (2012). Murphy (2014) showed that random temperature fluctuations can generate an extremely wide range of ice number densities. Since the low number density ice crystals are also associated with larger sizes, they sediment quickly and sweep out a much larger volume than that of the high number density ice crystals that stay aloft. Thus the rare temperature trajectories that result in the low-

ACPD
15, 35907–35938, 2015

est number densities are disproportionately important. They suggest the low mean and median observed ice number concentrations are caused by aircraft observations which usually measure low ice number density in this much larger volume.

In this study, we will examine the first two categories of proposals in a GCM to see if we are able to generate low ice number concentrations consistent with observations. We will not evaluate the third category related to ice sedimentation. Sedimentation of ice is included in the GCM (CAM5) that we use in this study. However, the vertical grid spacing (with 30 vertical layers) is not fine enough to capture the observed narrow layers of high ice crystal number concentrations with low ice crystal number concentration layers surrounding them (Jensen et al., 2013). For the first category of proposals, we will examine the effect of pre-existing ice and secondary organic aerosols (SOA) acting as IN. For the second category of proposals, we will examine three different representations of sub-grid updraft velocities in the ice nucleation parameterizations. For the first representation, we follow the suggestion by Spichtinger and Krämer (2013) and simply use the large-scale updraft velocity predicted by the GCM in the ice nucleation parameterization, excluding any effect from fast gravity waves. For the second representation, we use the sub-grid scale updraft velocity based on the fitted meso-scale temperature fluctuations from long-term aircraft temperature observations (Gary, 2006, 2008). This sub-grid scale updraft velocity was first introduced in a GCM by Wang and Penner (2010) and further studied by Wang et al. (2014). Wang et al. (2014) showed that using this updraft velocity produces a better hemispheric contrast in ice supersaturation compared to observations. The third representation is the sub-grid scale updraft velocity based on the modelled sub-grid scale turbulent kinetic energy (Neale et al., 2012; Gettelman et al., 2010). As shown in Fig. 1, this updraft velocity has the largest range. We will also examine the effect of using different mass accommodation coefficients (α) for water vapour deposition on ice crystals. This coefficient is not well known, with studies supporting values from 0.006 to unity (Magee et al., 2006; Skrotzki et al., 2013) and it has a significant impact on the predicted ice numbers (Zhang et al., 2013; Mur-

ACPD
15, 35907–35938, 2015

phy, 2014). The model and experiments are described in Sect. 2. Model results are presented in Sect. 3. Section 4 presents a summary and a short discussion.

2 Model and experiments

2.1 Description of the coupled CAM5/IMPACT model

We used the coupled CAM5/IMPACT model in this study. The CAM5/IMPACT model embeds the University of Michigan IMPACT chemistry and aerosol transport model as a module inside the Community Atmosphere Model version 5.3 (CAM5) (Zhou and Penner, 2014). CAM5 is the atmospheric component of the Community Earth System Model version 1.2 (CESM1.2). Readers are referred to Neale et al. (2012) and Liu et al. (2012a) for more model details. Here we briefly summarize the ice nucleation process. The default ice nucleation for cirrus clouds (below −35 °C) in CAM5 follows the parameterization developed by Liu and Penner (2005) (hereafter LP) and was implemented in CAM3 by Liu et al. (2007) and later in CAM5 by Gettelman et al. (2010). The LP parameterization treats the competition between homogenous freezing on sulphate haze droplets and heterogeneous nucleation on dust as well as other IN. We also tested the ice nucleation parameterization by Barahona and Nenes (2009) (hereafter BN). In this study, we used both parameterizations. The BN parameterization has the flexibility to use different water accommodation coefficients and different ice nucleation parameterizations for heterogeneous nucleation including those in Meyers et al. (1992) and Phillips et al. (2007, 2008) as well as the classical-nucleation-theory (CNT) (see Table 1 in Barahona and Nenes, 2009). The LP parameterization used the CNT based IN mechanism only and a fixed water accommodation coefficient equal to 0.1. To facilitate the comparison between the two parameterizations, we chose to use the CNT based IN mechanism in BN. In both ice nucleation parameterizations, up to 100 % of the potential IN are allowed to freeze when criteria for temperatures and supersaturations are met. The results from the LP parameterization are very similar to the results

ACPD
15, 35907–35938, 2015

from the BN parameterization when the water vapour accommodation coefficient is set to 0.1. So we only present the results from the BN parameterization here.

The IMPACT module runs in parallel with the default CAM5 aerosol module (MAM3) in CAM5 (Zhou and Penner, 2014). Aerosols simulated by the IMPACT module do not interact with any physical processe in CAM5 except in cirrus clouds (below −35 °C). In the ice nucleation parameterization sulphate particles and heterogeneous IN predicted by IMPACT replace those predicted by MAM3. The performance of the offline IMPACT model driven by CAM5 meteorological fields was previously evaluated by Zhou et al. (2012a, b) and was in good agreement with observations. The overall characteristics of the performance of the coupled IMPACT module within CAM5 are similar to this offline version. We present simulations using two versions of IMPACT, the basic version without secondary organic aerosols (SOA) and the version that includes SOA. The basic version simulates a total of 17 externally mixed aerosol types and/or size bins: 3 sizes representing the number and mass of pure sulphate aerosols (i.e. nucleation, Aitken and accumulation modes), 3 types of fossil/bio-fuel soot that depend on its hygroscopicity or the amount of sulphate on the soot particles, 2 aircraft soot modes (pre-activated in contrails or not), 1 biomass soot mode, 4 dust sizes, and 4 sea salt sizes. All these aerosols may mix with sulphate through condensation and coagulation processes or through sulphate formation in cloud drops. Thus, for all non-sulphate aerosols we also track the amount of sulphate mass coated on them. The SOA version includes the volatile organic compound (VOC) oxidation scheme implemented in Lin et al. (2012, 2014). It has approximately 129 separate gas-phase compounds (depending on which chemical oxidation scheme is used). It uses a chemical mechanism that includes both gas phase and aqueous or liquid phase production of SOA. Specifically, Glyoxal and methylglyoxal are dissolved into cloud and aqueous sulfate to form SOA, and some SOA is formed through the reactive uptake of epoxides on aqueous sulfate. Twenty different semi-volatile organic compounds (SVOCs), mainly consisting of organic nitrates and peroxides that are formed from gas phase VOC oxidations, are partitioned into the aerosol phase. In addition, when present within the aerosol phase,

ACPD
15, 35907–35938, 2015

the SVOCs form oligomers using a simplified scheme (Lin et al., 2012). In total, in addition to the 17 aerosol species in the basic version of IMPACT described above, the Lin et al. (2014) version separately follows a total of 35 additional low-volatility SOA species.

2.2 Experiment description

In the ice nucleation parameterization, we specify a single updraft velocity at each grid point. We used three different representations of the updraft: the grid resolved updraft velocity (WGRID), the updraft velocity derived from observed meso-scale temperature fluctuations as summarized by Gary (2006, 2008) (WGARY), and the updraft velocity based on the modelled sub-grid scale turbulent kinetic energy (WTKE). For each updraft representation, we used 4 different model set-ups, depending on whether heterogeneous nucleation (COMP), vapour deposition on pre-existing ice during ice nucleation (PRE), or SOA IN (SOA01) are included in the ice nucleation parameterization (COMP, COMP+SOA01, COMP+PRE and COMP+PRE+SOA01). In addition, for WGRID we added 2 other set-ups: a case with only homogeneous nucleation allowed (HOM) and a model set-up with vapour deposition on pre-existing ice during ice nucleation (HOM+PRE). Table 1 gives the definition of the set-ups for each updraft velocity category. Since we also vary the water vapour accommodation coefficient ($\alpha = 0.1$ or $\alpha = 1$), each set-up also includes a pair of simulations, one with $\alpha = 0.1$ and one with $\alpha = 1$. All cases use a horizontal resolution of $2.5^{\circ} \times 1.9^{\circ}$ and 30 vertical layers and are run for 6 years using year 2000 emissions. We chose to run the SOA capable version of the CAM/IMPACT model for only 2 years and to read-in the stored monthly averaged SOA fields from the second year for all cases, since the SOA capable version of the CAM/IMPACT model takes roughly 1.5 times more computer time than the basic version. The use of monthly averaged SOA fields does not significantly change the nature of the results. The output from the last 5 years of each simulation case is used in the analysis.

ACPD
15, 35907–35938, 2015

3 Results

3.1 Updraft velocities and SOA IN numbers

The updraft velocity plays a crucial role in ice nucleation. It determines how fast the RHi can grow and thus determines whether the RHi reaches the threshold for ice nucleation to occur after vapour deposition on newly formed ice begins. Figure 1a shows the probability density functions (PDFs) determined by sampling the updraft used during nucleation over tropical grids. Model results are sampled every 3 h from all grid points between 30° S to 30° N and below 87 hPa. The PDFs for the three different updraft velocities used here are shown for two different temperature ranges (185–205 K and 205–225 K). Results are from the COMP case in each updraft velocity category with $\alpha = 0.1$. The grid resolved large scale updraft velocity (WGRID) shows both negative and positive values varying between about −0.05 to 0.15 m s^{-1}. The magnitude of WGRID decreases as the temperature decreases (from 205–225 K to 185–205 K) or when the altitude increases. WGARY is the updraft velocity derived from the observed meso-scale temperature fluctuations, δT, and is a function of altitude, topography, season, and latitude (Gary, 2006, 2008). The observed temperature fluctuations were converted to sub-grid scale vertical velocities using

$$\text{WGARY (m s}^{-1}) = 0.23\delta T \text{ (K)}$$

following Kärcher and Burkhardt (2008) (aslo see Wang and Penner, 2010 and Wang et al., 2014). WGARY varies from 0.05 to 0.15 m s^{-1} and shows increased magnitudes as the temperature decreases with altitude. This increase is proportional to $p^{-0.4}$ (p is the pressure, see Eq. 3 in Gary, 2008) and is similar to the increase caused by the increase in the wave amplitudes required to conserve wave energy when the air density decreases with altitude. WTKE is the updraft velocity calculated from the modelled sub-grid turbulent kinetic energy (TKE) following Morrison and Pinto (2005):

$$\text{WTKE} = \sqrt{\frac{2}{3}\text{TKE}}$$

ACPD
15, 35907–35938, 2015

WTKE has the largest range of the three representations. It has a spike near zero which occurs when strong turbulence/convection is absent in a grid. The remaining portion of the PDF has a wide range from 0 to 2 m s^{-1}. Large updraft velocities, such as those at the higher end of this range produced from convection in the tropics, are accompanied by homogeneous freezing as we show later. Previously, an artificial upper limit of 0.2 m s^{-1} was used for WTKE in ice nucleation studies using the CAM5 model (Gettelman et al., 2010, 2012; Liu et al., 2012b; Zhang et al., 2013) to better reproduce observed in-cloud ice number concentrations. This upper limit was removed by Shi et al. (2015) after adding vapour deposition on pre-existing ice during ice nucleation. Here we also use the predicted updraft based on the TKE without any upper limit. We note that Shi et al. (2015) also limited the fraction of each grid cell that was allowed to undergo homogenous freezing. Here, we do not add this constraint.

During in-cloud ice nucleation, the updraft velocity (W) acts to increase the relative humidity by cooling the air parcel through adiabatic expansion while pre-existing ice particles act to decrease the relative humidity by consuming any water vapour above ice saturation. So mathematically, one can combine the effects of pre-existing ice particles and those from the cooling caused by the updraft velocity. This is equivalent to the use of a reduced updraft velocity while ignoring vapour deposition on pre-existing ice particles. This reduced updraft velocity is termed the effective updraft velocity (Kärcher et al., 2006; Shi et al., 2015). Figure 1b shows the PDFs of the three different updraft velocities and their effective updraft velocities in the temperature range 185–205 K sampled from grid points that only experience homogenous freezing. The effective updraft velocities shift to the left towards the smaller sizes. The effective WGRID PDF now only shows positive values since homogeneous freezing only occurs in grid boxes with updrafts that are positive and are cooling. Although the effective WTKE is significantly reduced, it still has a large fraction with values larger than 0.2 m s^{-1}.

In addition to the important role that the updraft velocity plays in ice nucleation, the concentrations of heterogeneous IN also play an important role by determining the competition between heterogeneous nucleation and homogeneous freezing. How-

ACPD
15, 35907–35938, 2015

ever, our understanding of which aerosol particles may serve as heterogeneous IN is still limited (Hoose and Möhler, 2012). Cziczo et al. (2013) showed that mineral dust dominates most measurements of the residual particles in ice crystals. Pratt et al. (2009) showed that ice-crystal residues from an aircraft measurement at high altitude over Wyoming are comprised mostly of biological particles (~ 33 %) and mineral dust (~ 50 %) with some minor contribution from soot (~ 4 %), salt (~ 4 %) and organic carbon/nitrate (~ 9 %). Lab studies show that activated fractions of Asian and Saharan desert dust can range from ~ 5–10 % at −20 °C to 20–40 % at temperatures colder than −40 °C (Field et al., 2006). In this study we assumed that 10 % of the total dust number can act as heterogeneous IN which is similar to the fractions suggested by Zhang et al. (2013) and Wang et al. (2014). For primary carbonaceous aerosols, we assume 0.1 % of hydrophilic fossil fuel soot, 0.05 % of hydrophobic fossil fuel soot (Koehler et al., 2009) and 0.1 % of total biomass burning soot (Möhler et al., 2005) are able to act as heterogeneous IN. For SOA, we lumped together all 35 SOA compounds together and assumed that 0.1 % of the total SOA could act as IN, similar to the fraction of biomass burning soot.

Figure 2 shows the annual zonal mean sulphate aerosol number concentration above 500 hPa in the Aitken and accumulation modes which are the number of particles able to freeze homogeneously. The number concentrations for different heterogeneous IN are also shown. The simulated sulphate number in the Aitken and accumulation modes (Fig. 2a) is of the order of 100 cm^{-3} in the tropical upper troposphere. The total IN without SOA (Fig. 2b) ranges from 0.5 to 30 L^{-1} in the upper troposphere. They are dominated by dust IN (Fig. 2d) with a minor contribution from biomass burning soot (Fig. 2e) below the tropopause. The contribution from fossil/bio fuel soot is even smaller and is largely negligible above 150 hPa. The number concentration of 0.1 % of SOA, which we treat here as IN, ranges 1 to 30 L^{-1} in the upper troposphere (Fig. 2c) and is about 2–5 times larger than the total background IN number without SOA above 200 hPa, except in the dust source and outflow regions near north Africa (not shown).

ACPD
15, 35907–35938, 2015

3.2 Results from WGRID cases

In this section, we examine the effect from water vapour deposition on pre-existing ice particles on ice crystal number concentrations when the grid resolved updraft velocity (WGRID) is used in the ice nucleation parameterization. We also examine the effect of including SOA as IN and of varying the water vapour accommodation coefficient. The use of the large-scale updraft velocity during ice nucleation is based on the parcel model study by Spichtinger and Krämer (2013). They showed that the superposition of large-scale updrafts and fast gravity waves would limit the ice nucleation time duration and thus the ice number. They showed that about 80 % of the observed ice spectrum could be explained by homogenous freezing while the remaining 20 % stem from heterogeneous and homogeneous freezing occurring within the same environment, and suggested that their parcel model results could be reproduced using only the large-scale updraft velocity. Here we test this theory using the GCM.

Figure 3 shows the simulated in-cloud ice number concentrations as a function of temperature from the WGRID cases. The top panel shows the results from the homogeneous freezing only cases and bottom panel shows the results from the homogeneous freezing/heterogeneous nucleation competition cases. The left and right panels show the results using two different water vapour accommodation coefficients (α = 0.1 and 1). The background blue shade shows the 25–75 % percentiles of observed in-cloud ice number concentrations compiled by Krämer et al. (2009). The solid curves show the 50 % percentiles of simulated ice number conentrations for each 1 K bin and the error bars show the 25–75 % percentiles. The model results were sampled every 3 h from 30° S to 75° N over tropical, mid-latitude and Arctic regions which include the observation locations reported in Krämer et al. (2009). Figure 3a shows that the HOM case overestimates the ice number contrentrations by more than one order of magnitude in cirrus clouds at temperatures less than 205 K but agrees better with observations in the temperature range from 205 to 220 K. When the effect of vapour deposition onto pre-existing ice is included, the effective WGRID (0–5 cm s^{-1}) is smaller than the origi-

ACPD
15, 35907–35938, 2015

nal WGRID (0–15 cm s^{-1}) for the grids with homogeneous freezing only (see Fig. 1b). Since a smaller updraft veclocity translates into a slower increase of RHi with time, fewer newly formed ice particles from homogeneous freezing are needed to reverse the growth of RHi and thus stall the further formation of particles from homogeneous freezing. In fact, if the number of pre-exisiting ice particles is large enough, homogeneous freezing may not even occur. As a result, the ice number concentration in the HOM+PRE case (blue curve) is substantially smaller than that from the HOM case, especially at lower temperatures (more than one order of magnitude). This case matches the observations of ice number concentration pretty well at temperatures less than 205 K, but underestimates concentrations at temperatures higher than 205 K. Figure 3b shows the results using a larger water vapour accommodation coefficient (α = 1). Since ice particles grow faster with the larger water vapour accommodation coefficient, the RHi grows more slowly. So fewer ice particles are formed. For the HOM case, the ice number concentrations are much smaller at lower temperatures (compare black curves in Fig. 3a and b). Case HOM+PRE (blue curves) also shows fewer ice particles but the difference between the case with α = 0.1 and 1.0 is relatively smaller.

Figure 3c shows the results from the cases that include the competition between homogeneous and heterogeneous nucleation. Compared to the HOM case in Fig. 3a, the COMP case in Fig. 3c shows smaller ice number concentrations, which is expected since the competition from heterogeneous nucleation, which can occur at lower RHi, reduces the occurrence frequencies of homogeneous freezing. The much larger concentrations of homogeneous freezing haze particles (see Fig. 2a) typically allow more ice to form than heterogeneous nucleation. When 0.1 % of SOA number is added as IN (case COMP+SOA01), there is a further reduction in the ice number concentration, especially at lower temperatures. But at higher temperatures (T > 205 K) the change is relatively smaller. This is because at higher temperatures (T > 205 K) ice grows faster than at lower temperatures thus the effect of any additional IN (SOA IN here) is diminished. When vapour deposition onto pre-existing ice is included (case COMP+PRE), the effect on ice number is much larger than the case for the addition of SOA IN. The

ACPD
15, 35907–35938, 2015

predicted ice number concentrations in this case are of the order of 10 L^{-1}, which is comparable to the SOA IN number (about 10 L^{-1} as shown in Fig. 2c). The SOA IN require an RHi of about 120 % to nucleate and start to consume the water vapour, while the pre-existing ice particles, if present, can start to consume the excess water vapour as long as the RHi is above 100 %. So the pre-existing ice particles are more effective at reducing the RHi and suppressing ice nucleation by homogeneous and/or heterogeneous nucleation. In case COMP+PRE, since the effective WGRID is small, homogeneous freezing is almost completely suppressed. Further adding SOA IN to case COMP+PRE+SOA01 only decreases the ice number at the coldest temperatures (< 195 K). When a larger water vapor accommodation coefficient ($\alpha = 1$) is used (Fig. 3d), SOA IN are more effective at reducing the ice number at the coldest temperatures (see the pink curve at $T < 195$ K in Fig. 3d) but become less important when vapour deposition onto pre-existing ice is included.

All in all, for cases using the large-scale grid resolved updraft velocity, as long as vapour deposition onto pre-exising ice is included, both the homogeneous freezing only case (HOM) and the competition cases (COMP) can produce in-cloud ice numbers in good agreement with the observations in the TTL cirrus clouds at temperatures less than 205 K. If vapour deposition onto pre-existing ice during ice nucleation is not considered, then a larger water vapour accommodation coefficient ($\alpha = 1$) together with SOA as IN can also lead to a good agreement with observations.

3.3 Results from WGARY cases

Figure 4 shows the results from the cases that include homogeneous/heterogeneous competition using WGARY as the sub-grid scale updraft velocity in the ice nucleation parameterization. Results from the COMP case compare well with the observations in warm cirrus clouds in the temperature range from 205 to 220 K for both water vapour accommodation coefficients. However, these cases overestimate number concentrations at temperatures less than 205 K. Similar to the results in Fig. 3, including vapour

ACPD
15, 35907–35938, 2015

deposition onto pre-existing ice can effectively reduce the in-cloud ice number concentrations. This leads to underestimated ice number concentrations in warmer cirrus. But unlike the results from the WGRID cases in Fig. 3, for this intermediate range updraft velocity (WGARY from 0.05–0.15 m s^{-1} in Fig. 1), the inclusion of vapour deposition onto pre-existing ice alone is not able to explain the observed low ice number concentrations in cold cirrus clouds ($T < 205$ K). Adding SOA IN (red curves in Fig. 4) further reduces the in-cloud ice number concentrations at the lowest temperatures especially if $\alpha = 1$. Adding SOA without including pre-existing ice (pink curves in Fig. 4) is not very effective at the lowest temperatures unless $\alpha = 1$. The best prediction of ice number concentrations in cold cirrus clouds ($T < 205$ K) is from case COMP+PRE+SOA01 (red curve in Fig. 4b) when the effects from the pre-existing ice particles, a larger water vapor accommodation coefficient ($\alpha = 1$) and SOA IN are all included. At higher temperatures ($T > 210$ K) there is a slight increase of ice number concentration when adding SOA in the pre-existing ice case, which suggests heterogeneous nucleation already dominates in this temperature regime, so that the addition of SOA IN acts to increase ice numbers.

3.4 Results from WTKE cases

Figure 5 shows the results from cases with both heterogeneous and homogenous nucleation (COMP) when the updraft velocity (WTKE) is based on the sub-grid scale turbulent kinetic energy. As WTKE is on average much higher than the other two velocity cases, the COMP cases without vapour deposition onto pre-existing ice overestimate the ice numbers substantially for both water vapor accommodation coefficients. Adding SOA IN has almost no effect on the simulated ice number concentrations except at higher temperatures around 220 K (pink curve in Fig. 5a). The critical IN number needed to suppress homogeneous freezing increases with decreased temperature and increased updraft velocities. This suggests that when WTKE is used, the addition of 0.1 % of the total SOA as IN is not large enough to reach this critical IN number (except at some of the temperatures higher than 215 K) (see pink curve in Fig. 5a). If 1 % of the

ACPD
15, 35907–35938, 2015

total SOA is allowed to act as IN, then there are significant decreases in the ice number concentrations at temperatures above 205 K (see pink curves in Fig. S1 in the Supplement). But the effect is still small at the lowest temperatures. When vapor deposition onto pre-exisiting ice is included, the WTKE is reduced but is still quite large compared to WGARY (see Fig. 1b). The simulated ice numbers from the COMP+PRE case are reduced by almost one order of magnitude and compare well with observations in cirrus clouds at temperatures warmer than 205 K for both water vapour accommodation coefficients. Since the effective WTKE is smaller than the original WTKE, SOA IN are able to reduce some of the occurrences of homogenous freezing at temperatures as low as 205 K (see red curve in Fig. 5a). But overall the effect from the added SOA IN is small and not effective in reducing the ice number concentration for these larger updraft velocities. Similar reusults have been reported in a geoengingeering study by Penner et al. (2015) when WTKE is used and 0.1 % or 0.5 % of total SOA is added as IN (see their Fig. 2).

4 Conclusion and discussion

In this study, we examined the effect from three different updraft velocities and two different water vapor accommodation coefficients (α = 0.1 or 1) used in ice nucleation parameterizations. We also examined the effect of including vapour deposition onto pre-existing ice particles during ice nucleation and the effect of including SOA as heterogeneous IN. The different simulations were compared to observed in-cloud ice number concentrations in cirrus clouds. The simulated in-cloud ice number is shown to strongly depend on the magnitude of the updraft velocity since this determines the occurrence frequency of homogenous freezing. Inclusion of vapour deposition onto pre-existing ice during nucleation or increasing the water vapor accommodation coefficient (from 0.1 to 1) can both effectively reduce the simulated ice numbers. The effect from SOA acting as IN is more complex since it depends on the background ice nucleation mechanism and whether or not the effect of pre-existing ice is included. Overall, SOA IN are most

ACPD
15, 35907–35938, 2015

effective at suppressing homogenous freezing and thus reducing ice numbers when updraft velocities are intermediate in magnitude (e.g. WGARY from 0.05–0.15 m s^{-1}). Including the effect of pre-existing ice reduces the effect of SOA IN. For small updraft velocities (e.g. WGRID), SOA IN are effective at reducing ice numbers only at lower temperatures. For large updraft velocities (e.g. WTKE), SOA IN only show a small effect at higher temperatures.

Here is a summary of the set-ups for different updraft velocities needed to produce ice number concentrations in-line with observations at temperatures less than 205 K:

1. For the small grid resolved updraft velocities (i.e., case WGRID where W is typically < 0.1 m s^{-1}), using either homogenous freezing only or including the competition between homogeneous and heterogeneous nucleation in the ice nucleation parameterization is able to produce the observed lower ice numbers when vapour deposition onto pre-existing ice particles is considered. When vapour deposition onto pre-existing ice particles is not considered, then a larger water vapour accommodation coefficient ($\alpha = 1$) and SOA IN are both needed to produce the observed lower ice numbers.

2. For intermediate velocities (e.g., WGARY with W varying from 0.05–0.15 m s^{-1}), the effects from vapour deposition onto pre-existing ice particles, a larger water vapour accommodation coefficient ($\alpha = 1$), and SOA IN are all needed to produce the observed lower ice numbers.

3. For the larger updraft velocities (such as those found in WTKE which vary up to 2 m s^{-1}), all set-ups overestimate the in-cloud ice numbers.

Thus, from our study, one can only use WGRID and WGARY to reproduce in-cloud ice numbers in-line with observations at temperatures less than 205 K. But these simulations underestimate the ice number at temperatures higher than 205 K. On the other hand, even though no set-up for WTKE is able to reproduce in-cloud ice numbers in-line with observations at temperatures less than 205 K, the results agree best with

ACPD
15, 35907–35938, 2015

observations at temperatures higher than 205 K. No simple tuning of the ice nucleation parameters or set-up can form ice number concentrations that fit both temperature ranges. The obvious issue is that ice numbers from the model and the observations have nearly opposite temperature dependence slopes (i.e., decreased ice number with increased temperature seen from models vs. increased ice number with increased temperature seen from observations), a point noted previously using parcel model studies (Murphy, 2014). The slope seen from the model results is a fundamental consequence of slower growth rate of ice particles and less water vapour available at lower temperatures. The only way to reverse the slope would be if some parameters, such as IN concentrations or sub-grid updraft velocity, were themselves functions of temperature. It is possible that CAM5 may overestimate the TKE in the upper troposphere at temperatures less than 205 K, but an analysis of this is beyond the scope of this paper. When we use WGRID at temperatures lower than 205 K and WTKE at temperatures higher than 205 K, we are able to reverse the slope and the simulated ice number concentrations fit the observations well in both temperature ranges (see Fig. 6). But this choice of updraft velocity lacks any theory or observational support. It might be that we could only apply the proposal by Spichtinger and Krämer (2013) of using the large-scale updraft in the ice nucleation parameterization at temperatures lower than 205 K but not at temperatures higher than 205 K. The dynamic conditions near the top of troposphere may favour a combination of a slow persistent large-scale updraft velocity and short gravity waves which satisfy the special situation described by Spichtinger and Krämer (2013) in which the ice number formed from the short gravity waves is limited; while at lower altitudes, short gravity waves effect may not be limited due to higher large-scale updraft velocities. Another possibility might be that SOA number concentrations only become glassy and act as IN at temperatures less than 205 K. However, while this model setup allows us to improve crystal concentrations below 205 K, it does not produce a reversed slope.

ACPD
15, 35907–35938, 2015

The Supplement related to this article is available online at doi:10.5194/acpd-15-35907-2015-supplement.

Acknowledgements. This work was supported by the NSF under grants AGS-0946739 and AGS-1540954. We acknowledge high-performance computing support from Yellowstone (http://n2t.net/ark:/85065/d7wd3xhc) provided by NCAR's Computational and Information Systems Laboratory and sponsored by the National Science Foundation.

References

Abbatt, J. P. D., Benz, S., Cziczo, D. J., Kanji, Z., Lohmann, U., and Möhler, O.: Solid ammonium sulfate aerosols as ice nuclei: a pathway for cirrus cloud formation, Science, 313, 1770–1773, doi:10.1126/science.1129726, 2006.

Barahona, D. and Nenes, A.: Parameterization of cirrus formation in large scale models: Homogenous nucleation, J. Geophys. Res., 113, D11211, doi:10.1029/2007JD009355, 2008.

Barahona, D. and Nenes, A.: Parameterizing the competition between homogeneous and heterogeneous freezing in ice cloud formation – polydisperse ice nuclei, Atmos. Chem. Phys., 9, 5933–5948, doi:10.5194/acp-9-5933-2009, 2009.

Barahona, D. and Nenes, A.: Dynamical states of low temperature cirrus, Atmos. Chem. Phys., 11, 3757–3771, doi:10.5194/acp-11-3757-2011, 2011.

Cziczo, D. J., Froyd, K. D., Hoose, C., Jensen, E. J., Diao, M., Zondlo, M. A., Smith, J. B., Twohy, C. H., and Murphy, D. M.: Clarifying the dominant sources and mechanisms of cirrus cloud formation, Science, 340, 1320–1324, doi:10.1126/science.1234145, 2013.

Dinh, T., Podglajen, A., Hertzog, A., Legras, B., and Plougonven, R.: Effect of gravity wave temperature fluctuations on homogeneous ice nucleation in the tropical tropopause layer, Atmos. Chem. Phys. Discuss., 15, 8771–8799, doi:10.5194/acpd-15-8771-2015, 2015.

Field, P. R., Möhler, O., Connolly, P., Krämer, M., Cotton, R., Heymsfield, A. J., Saathoff, H., and Schnaiter, M.: Some ice nucleation characteristics of Asian and Saharan desert dust, Atmos. Chem. Phys., 6, 2991–3006, doi:10.5194/acp-6-2991-2006, 2006.

Gary, B. L.: Mesoscale temperature fluctuations in the stratosphere, Atmos. Chem. Phys., 6, 4577–4589, doi:10.5194/acp-6-4577-2006, 2006.

ACPD

15, 35907–35938, 2015

Gary, B. L.: Mesoscale temperature fluctuations in the Southern Hemisphere stratosphere, Atmos. Chem. Phys., 8, 4677–4681, doi:10.5194/acp-8-4677-2008, 2008.
Gettelman, A., Liu, X., Ghan, S. J., Morrison, H., Park, S., Conley, A. J., Klein, S. A., Boyle, J., Mitchell, D. L., and Li, J. L. F.: Global simulations of ice nucleation and ice supersaturation with an improved cloud scheme in the Community Atmosphere Model, J. Geophys. Res.-Atmos., 115, D18216, doi:10.1029/2009jd013797, 2010.
Gettelman, A., Liu, X., Barahona, D., Lohmann, U., and Chen, C.: Climate impacts of ice nucleation, J. Geophys. Res.-Atmos., 117, D20201, doi:10.1029/2012jd017950, 2012.
Hoose, C. and Möhler, O.: Heterogeneous ice nucleation on atmospheric aerosols: a review of results from laboratory experiments, Atmos. Chem. Phys., 12, 9817–9854, doi:10.5194/acp-12-9817-2012, 2012.
Jensen, E. J., Toon, O. B., Selkirk, H. B., Spinhirne, J. D., and Schoeberl, M. R.: On the formation and persistence of subvisible cirrus clouds near the tropical tropopause, J. Geophys. Res., 101, 21361–21375, 1996.
Jensen, E. J., Pfister, L., Bui, T.-P., Lawson, P., and Baumgardner, D.: Ice nucleation and cloud microphysical properties in tropical tropopause layer cirrus, Atmos. Chem. Phys., 10, 1369–1384, doi:10.5194/acp-10-1369-2010, 2010.
Jensen, E. J., Pfister, L., and Bui, T. P.: Physical processes controlling ice concentrations in cold cirrus near the tropical tropopause, J. Geophys. Res., 117, D11205, doi:10.1029/2011JD017319, 2012.
Jensen, E. J., Diskin, G., Lawson, R. P., Lance, S., Bui, T. P., Hlavka, D., McGill, M., Pfister, L., Toon, O. B., and Gao, R.: Ice nucleation and dehydration in the Tropical Tropopause Layer, P. Natl. Acad. Sci., 110, 2041–2046, doi:10.1073/pnas.1217104110, 2013.
Kärcher, B. and Burkhardt, U.: A cirrus cloud scheme for general circulation models, Q. J. Roy. Meteor. Soc., 134, 1439–1461, doi:10.1002/Qj.301, 2008.
Kärcher, B. and Ström, J.: The roles of dynamical variability and aerosols in cirrus cloud formation, Atmos. Chem. Phys., 3, 823–838, doi:10.5194/acp-3-823-2003, 2003.
Kärcher, B., Hendricks, J., and Lohmann, U.: Physically based parameterization of cirrus cloud formation for use in global atmospheric models, J. Geophys. Res., 111, D01205, doi:10.1029/2005JD006219, 2006.
Koehler, K. A., DeMott, P. J., Kreidenweis, S. M., Popovicheva, O. B., Petters, M. D., Carrico, C. M., Kireeva, E. D., Khokhlovac, T. D., and Shonijac, N. K.: Cloud condensation nuclei

ACPD
15, 35907–35938, 2015

and ice nucleation activity of hydrophobic and hydrophilic soot particles, Phys. Chem. Chem. Phys., 11, 7906–7920, doi:10.1039/b905334b, 2009.
Koop, T., Luo, B., Tsias, A., and Peter, T.: Water activity as the determinant for homogeneous ice nucleation in aqueous solutions, Nature, 406, 611–614, 2000.
Krämer, M., Schiller, C., Afchine, A., Bauer, R., Gensch, I., Mangold, A., Schlicht, S., Spelten, N., Sitnikov, N., Borrmann, S., de Reus, M., and Spichtinger, P.: Ice supersaturations and cirrus cloud crystal numbers, Atmos. Chem. Phys., 9, 3505–3522, doi:10.5194/acp-9-3505-2009, 2009.
Kuebbeler, M., Lohmann, U., Hendricks, J., and Kärcher, B.: Dust ice nuclei effects on cirrus clouds, Atmos. Chem. Phys., 14, 3027–3046, doi:10.5194/acp-14-3027-2014, 2014.
Lin, G., Penner, J. E., Sillman, S., Taraborrelli, D., and Lelieveld, J.: Global modeling of SOA formation from dicarbonyls, epoxides, organic nitrates and peroxides, Atmos. Chem. Phys., 12, 4743–4774, doi:10.5194/acp-12-4743-2012, 2012.
Lin, G., Sillman, S., Penner, J. E., and Ito, A.: Global modeling of SOA: the use of different mechanisms for aqueous-phase formation, Atmos. Chem. Phys., 14, 5451–5475, doi:10.5194/acp-14-5451-2014, 2014.
Liu, X. and Penner, J. E.: Ice nucleation parameterization for a global model, Meteorol. Z., 14, 499–514, 2005.
Liu, X., Penner, J. E., Ghan, S. J., and Wang, M.: Inclusion of ice microphysics in the NCAR community atmospheric model version 3 (CAM3), J. Climate, 20, 4526–4547, doi:10.1175/JCLI4264.1, 2007.
Liu, X., Easter, R. C., Ghan, S. J., Zaveri, R., Rasch, P., Shi, X., Lamarque, J.-F., Gettelman, A., Morrison, H., Vitt, F., Conley, A., Park, S., Neale, R., Hannay, C., Ekman, A. M. L., Hess, P., Mahowald, N., Collins, W., Iacono, M. J., Bretherton, C. S., Flanner, M. G., and Mitchell, D.: Toward a minimal representation of aerosols in climate models: description and evaluation in the Community Atmosphere Model CAM5, Geosci. Model Dev., 5, 709–739, doi:10.5194/gmd-5-709-2012, 2012a.
Liu, X., Shi, X., Zhang, K., Jensen, E. J., Gettelman, A., Barahona, D., Nenes, A., and Lawson, P.: Sensitivity studies of dust ice nuclei effect on cirrus clouds with the Community Atmosphere Model CAM5, Atmos. Chem. Phys., 12, 12061–12079, doi:10.5194/acp-12-12061-2012, 2012b.

ACPD
15, 35907–35938, 2015

Magee, N., Moyle, A. M., and Lamb, D.: Experimental determination of the deposition coefficient of small cirrus-like ice crystals near 50 °C, Geophys. Res. Lett., 33, L17813, doi:10.1029/2006GL026665, 2006.
Meyers, M. P., DeMott, P. J., and Cotton, R.: New primary ice nucleation parameterization in an explicit cloud model, J. Appl. Meteorol., 31, 708–721, 1992.
Möhler, O., Büttner, S., Linke, C., Schnaiter, M., Saathoff, H., Stetzer, O., Wagner, R., Krämer, M., Mangold, A., Ebert, V., and Schurath, U.: Effect of sulfuric acid coating on heterogeneous ice nucleation by soot aerosol particles, J. Geophys. Res., 110, D11210, doi:10.1029/2004JD005169, 2005.
Morrison, H. and Pinto, J. O.: Mesoscale modeling of springtime arctic mixed-phase stratiform clouds using a new two-moment bulk microphysics scheme, J. Atmos. Sci., 62, 3683–3704, 2005.
Murphy, D. M.: Rare temperature histories and cirrus ice number density in a parcel and a one-dimensional model, Atmos. Chem. Phys., 14, 13013–13022, doi:10.5194/acp-14-13013-2014, 2014.
Murray, B., Wilson, T. W., Dobbie, S., Cui, Z., Al-Jumur, S. M. R. K., Möhler, O., Schnaiter, M., Wagner, R., Benz, S., Niemand, M., Saathoff, H., Ebert, V., Wagner, S., and Kärcher, B.: Heterogeneous nucleation of ice particles on glassy aerosols under cirrus conditions, Nat. Geosci., 3, 233–237, doi:10.1038/NGEO817, 2010.
Neale, R. B., Gettelman, A., Park, S., Conley, A. J., Kinnison, D., Marsh, D., Smith, A. K., Vitt, F., Morrison, H., Cameron-Smith, P., Collins, W. D., Iacono, M. J., Easter, R. C., Liu, X., and Taylor, M. A.: Description of the NCAR Community Atmosphere Model (CAM 5.0), NCAR Tech. Note NCAR/TN-485CSTR, Natl. Cent. for Atmos. Res., Boulder, CO, USA, 289 pp., 2012.
Penner, J. E., Zhou, C., and Liu, X.: Can cirrus cloud seeding be used for geoengineering?, Geophys. Res. Lett., 42, 8775–8782, doi:10.1002/2015GL065992, 2015.
Phillips, V. T. J., Donner, L. J., and Garner, S. T.: Nucleation processes in deep convection simulated by a cloud-system-resolving model with double-moment bulk microphysics, J. Atmos. Sci., 64, 738–761, doi:10.1175/JAS3869.1, 2007.
Phillips, V. T. J., DeMott, P. J., and Andronache, C.: An empirical parameterization of heterogeneous ice nucleation for multiple chemical species of aerosol, J. Atmos. Sci., 65, 2757–2783, doi:10.1175/2007JAS2546.1, 2008.

ACPD
15, 35907–35938, 2015

Pratt, K., DeMott, P., French, J., Wang, Z., Westphal, D., Heyms-field, A., Twohy, C., Prenni, A., and Prather, K.: In situ detection of biological particles in cloud ice-crystals, Nat. Geosci., 2, 398–401, 2009.
Pruppacher, H. R. and Klett, J. D.: Microphysics of Clouds and Precipitation, Atmospheric and Oceanographic Sciences Library, Kluwer Academic Publishers, Dordrecht, the Netherlands, 1997.
Ramanathan, V. and Collins, W.: Thermodynamic regulation of ocean warming by cirrus clouds deduced from observations of the 1987 El-Nino, Nature, 351, 27–32, 1991.
Rogers, D. C., DeMott, P. J., Kreidenweis, S. M., and Chen, Y.: Measurements of ice nucleating aerosols during SUCCESS, Geophys. Res. Lett., 25, 1383–1386, doi:10.1029/97GL03478, 1998.
Rossow, W. B. and Schiffer, R. A.: Advances in understanding clouds from ISCCP, B. Am. Meteorol. Soc., 80, 2261–2287, 1999.
Shi, X., Liu, X., and Zhang, K.: Effects of pre-existing ice crystals on cirrus clouds and comparison between different ice nucleation parameterizations with the Community Atmosphere Model (CAM5), Atmos. Chem. Phys., 15, 1503–1520, doi:10.5194/acp-15-1503-2015, 2015.
Skrotzki, J., Connolly, P., Schnaiter, M., Saathoff, H., Möhler, O., Wagner, R., Niemand, M., Ebert, V., and Leisner, T.: The accommodation coefficient of water molecules on ice – cirrus cloud studies at the AIDA simulation chamber, Atmos. Chem. Phys., 13, 4451–4466, doi:10.5194/acp-13-4451-2013, 2013.
Spichtinger, P. and Krämer, M.: Tropical tropopause ice clouds: a dynamic approach to the mystery of low crystal numbers, Atmos. Chem. Phys., 13, 9801–9818, doi:10.5194/acp-13-9801-2013, 2013.
Wang, M. and Penner, J. E.: Cirrus clouds in a global climate model with a statistical cirrus cloud scheme, Atmos. Chem. Phys., 10, 5449–5474, doi:10.5194/acp-10-5449-2010, 2010.
Wang, M., Liu, X., Zhang, K., and Comstock, J. M.:Aerosol effects on cirrus through ice nucleation in the Community Atmosphere Model CAM5 with a statistical cirrus scheme, J. Adv. Model. Earth Syst., 6, 756–776, doi:10.1002/2014MS000339, 2014.
Wang, P. H., Minnis, P., McCormick, M. P., Kent, G. S., and Skeens, K. M.: A 6 year climatology of cloud occurrence frequency from stratospheric aerosol and gas experiment II observations (1985–1990), J. Geophys. Res., 101, 29407–29429, 1996.
Wylie, D. P. and Menzel, W. P.: Eight years of high cloud statistics using HIRS, J. Climate, 12, 170–184, 1999.

ACPD
15, 35907–35938, 2015

Zhang, K., Liu, X., Wang, M., Comstock, J. M., Mitchell, D. L., Mishra, S., and Mace, G. G.: Evaluating and constraining ice cloud parameterizations in CAM5 using aircraft measurements from the SPARTICUS campaign, Atmos. Chem. Phys., 13, 4963–4982, doi:10.5194/acp-13-4963-2013, 2013.

Zhou, C. and Penner, J. E.:Aircraft soot indirect effect on large-scale cirrus clouds: Is the indirect forcing by aircraft soot positive or negative?, J. Geophys. Res.-Atmos., 119, 11303–11320, doi:10.1002/2014JD021914, 2014.

Zhou, C., Penner, J. E., Ming, Y., and Huang, X. L.: Aerosol forcing based on CAM5 and AM3 meteorological fields, Atmos. Chem. Phys., 12, 9629–9652, doi:10.5194/acp-12-9629-2012, 2012a.

Zhou, C., Penner, J. E., Flanner, M. G., Bisiaux, M. M., Edwards, R., and McConnell, J. R.: Transport of black carbon to polar regions: sensitivity and forcing by black carbon, Geophys. Res. Lett., 39, L22804, doi:10.1029/2012GL053388, 2012b.

ACPD
15, 35907–35938, 2015

Table 1. Description of the experiments.

Case name	Case description
HOM*	Only homogeneous freezing in the ice nucleation parameterization.
HOM+PRE*	Only homogeneous freezing in the ice nucleation parameterization; pre-existing ice effect in the ice nucleation parameterization.
COMP	Competition between homogeneous freezing and heterogeneous nucleation.
COMP+SOA01	Competition between homogeneous freezing and heterogeneous nucleation; 0.1 % of SOA acting as heterogeneous IN.
COMP+PRE	Competition between homogeneous freezing and heterogeneous nucleation; pre-existing ice effect in the ice nucleation parameterization.
COMP+PRE+SOA01	Competition between homogeneous freezing and heterogeneous nucleation; pre-existing ice effect in the ice nucleation parameterization; 0.1 % of SOA acting as heterogeneous IN.

* Case HOM and HOM+PRE are for WGRID only.

ACPD
15, 35907–35938, 2015

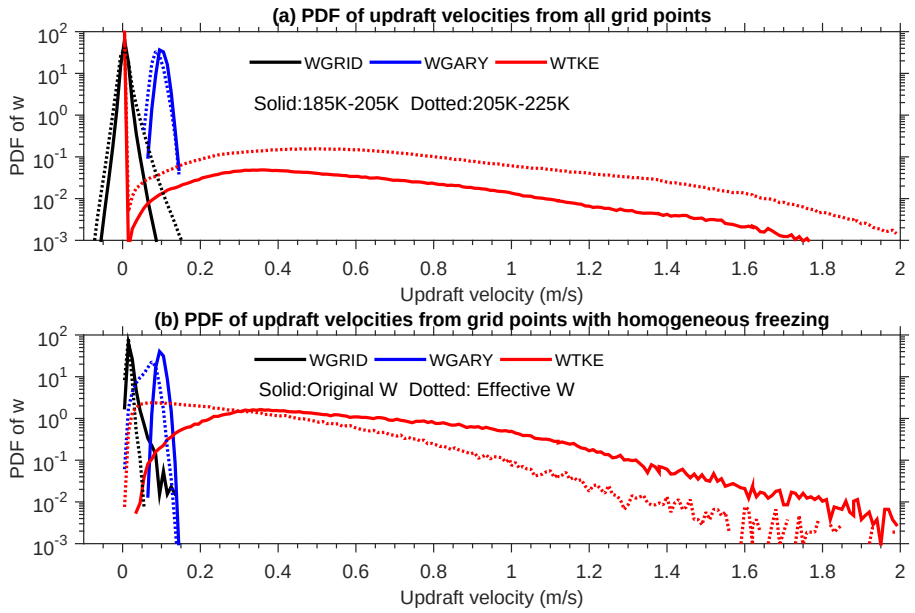

Figure 1. (a) Probability density functions (PDFs) of updraft velocity for three different representations (black: large-scale W, blue: meso-scale W from Gary, 2006, 2008, red: TKE based subgrid W) from all grid points in two temperature ranges. **(b)** Probability density functions of updraft velocity for the three different updraft velocity representations from grid points with homogenous freezing only in the temperature range 185–205 K. Solid curves are the original W and dotted curves are the effective W after accounting for vapour deposition onto pre-existing ice. Model results are sampled every 3 h below 87 hPa.

ACPD
15, 35907–35938, 2015

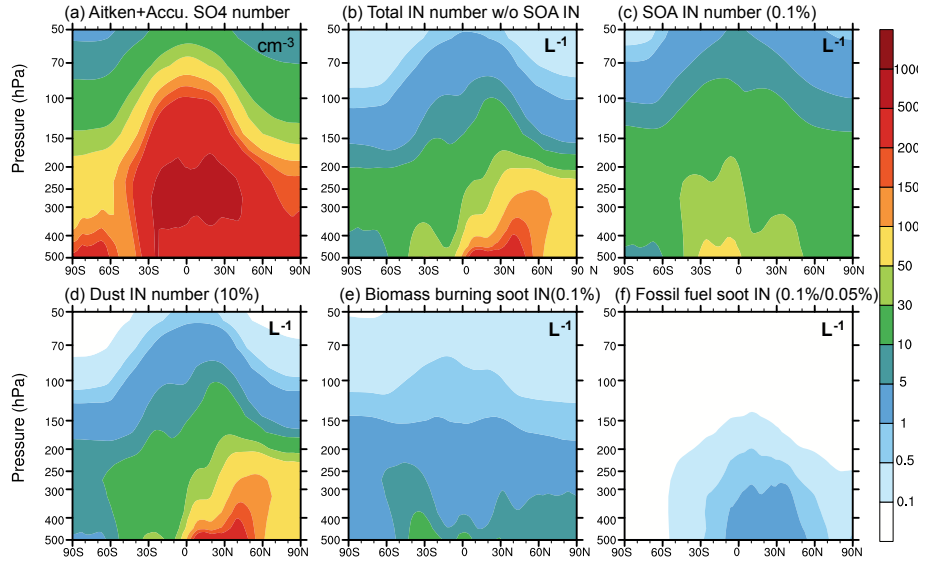

Figure 2. (a) Aitken and accumulation mode sulfate number (cm^{-3}). **(b)** Total background heterogeneous IN number (L^{-1}) without SOA IN: i.e. the sum of panels **(d–f)**. **(c)** SOA IN number (L^{-1}): 0.1 % of the total SOA number. **(d)** Dust IN number (L^{-1}): 10 % of the total dust number. **(e)** Biomass burning soot IN number (L^{-1}): 0.1 % of total biomass buring soot number. **(f)** Fossil fuel soot IN number (L^{-1}): 0.1 % of hydrophilic fossil fuel soot and 0.05 % of hydrophobic fossil fuel soot.

ACPD
15, 35907–35938, 2015

What controls the low ice number concentration in the upper troposphere?

C. Zhou et al.

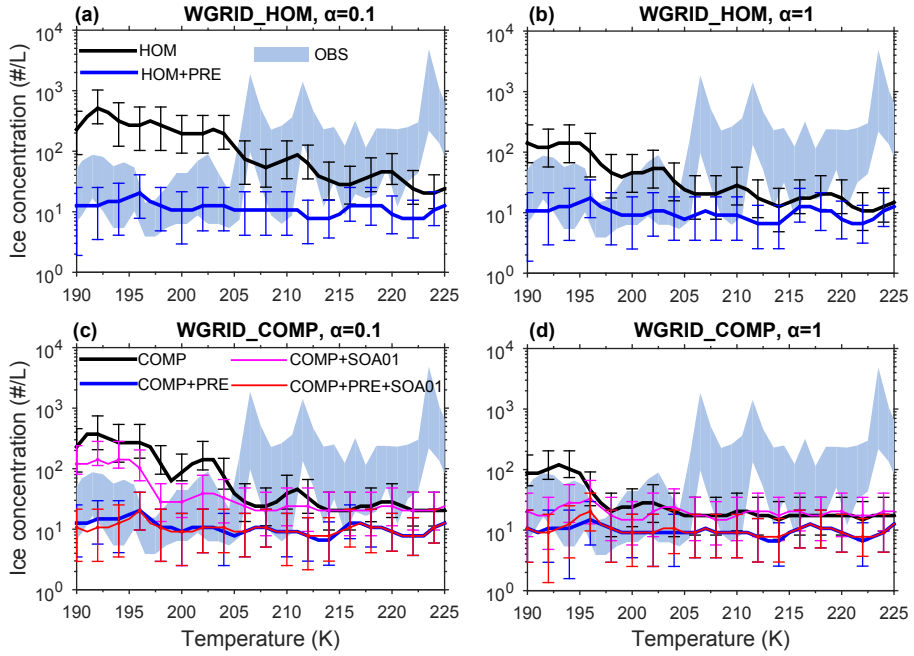

Figure 3. In-cloud ice crystal number concentration ($\#\,L^{-1}$) vs. temperature from cases using the grid resolved updraft velocity (WGRID) in the ice nucleation parameterization. Solid lines show the 50 % percentile values for each 1 K bin. Error bars show the 25–75 % percentiles. Background shaded regions show the 25–75 % percentiles from observations compiled by Krämer et al. (2009). Upper panel shows the results from the homogeneous freezing only cases and bottom panel shows the results from the competition cases. Left panel shows the results from cases with water vapor accommodation coefficient α = 0.1. Right panel shows the results from cases with water vapor accommodation coefficient α = 1. Model results are sampled every 3 h from 30° S to 75° N over tropical, mid-latitude and Arctic regions which includes the observation locations reported in Krämer et al. (2009).

ACPD
15, 35907–35938, 2015

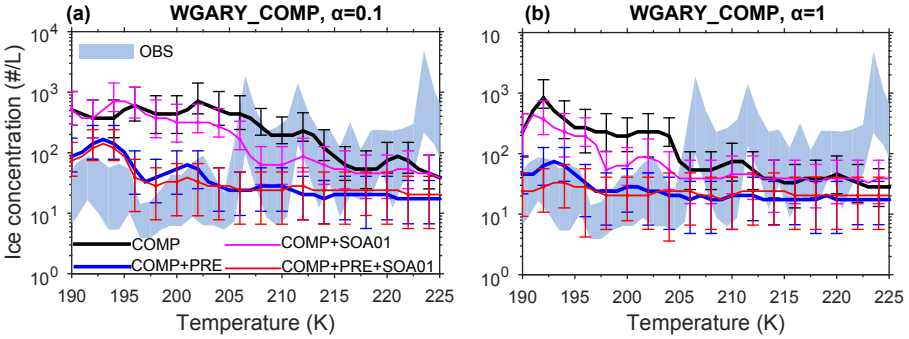

Figure 4. Same as Fig. 3c and d except the updraft velocity (WGARY) derived from the observed meso-scale temperature fluctuations from Gary (2006, 2008) was used in the ice nucleation parameterization.

ACPD
15, 35907–35938, 2015

What controls the low ice number concentration in the upper troposphere?

C. Zhou et al.

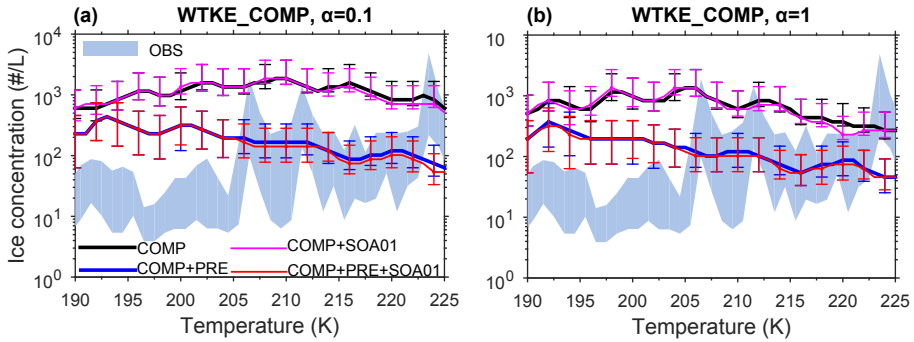

Figure 5. Same as Fig. 3c and d except the sub-grid scale tubulent kinetic energy based updraft velocity (WTKE) was used in the ice nucleation parameterization.

ACPD
15, 35907–35938, 2015

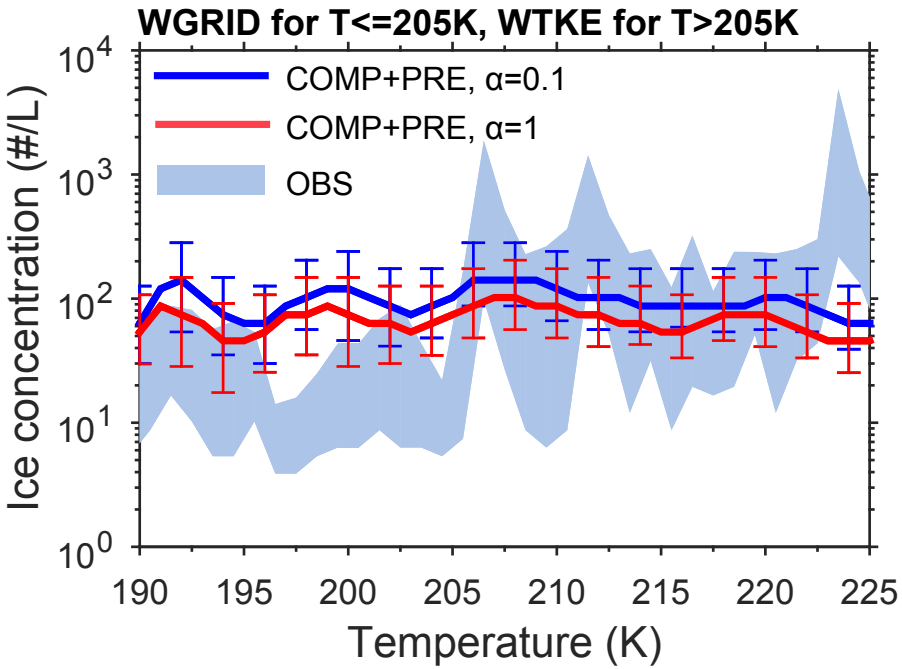

Figure 6. In-cloud ice crystal number concentration ($\#L^{-1}$) vs. temperature from two COMP+PRE cases using WGRID for temperature less than or equal to 205 K and WTKE for temperature higher than 205 K in the ice nucleation parameterization. Blue curve is from the case with water vapor accommodation coefficient $\alpha = 0.1$ and the red curve is from the case with water vapor accommodation coefficient $\alpha = 1$.

ACPD
15, 35907–35938, 2015